Comparative Analysis on Metamaterial based Microstrip Patch Antenna on Square and Triangular Patch

Divya Shrivastava[1] Sunil Kumar Singh[2]
[1,2]Department of Electronics & Telecommunication Engineering
[1,2]Jabalpur Engineering College Jabalpur Madhya Pradesh- 482011 India

Abstract— Two antenna structures loaded with S-shape loaded reactive impedance surface (S-RIS) square and equilateral triangular shapes are designed and studied. The square Microstrip patch antenna is found to be resonant at two frequencies 4.8 and 6.8GHz in C-band. In the case of S-RIS loaded triangle it is resonant with high bandwidth in the frequency range of 7- 9.2GHz covering C-band and X-band frequencies respectively. This structure showed resonance at 7.6 GHz. The directive gain for S-RIS square Microstrip patch antenna is 5.9dBi at 4.8GHz whereas for S-RIS triangle Microstrip patch antenna the directive gain at 8.1GHz is 5.53dBi. It has been observed that both structures showed high gain at resonance frequencies. Square shape is resonant at two frequencies while triangular patch is resonant only one frequency with high bandwidth and gain. Both designs show miniaturization and high performance. Due to miniaturization and gain considerations proposed designs can be used to design and fabricate a phased array antenna for synthetic aperture radar (SAR) for dual band and high bandwidth applications. The simulation was performed in Computer Simulation Technology.

Key words: Metamaterial, Antenna Miniaturization, Reactive-Impedance Surface (RIS), Patch Antennas, Return Loss

I. INTRODUCTION

Metamaterial was developed in 1967 by Russian theorist Victor Veselago. In his paper, Veselago stated that although LH materials do not exist in nature, they can be artificially constructed. Veselago concluded that the realization of a LH Metamaterial will be possible with the discovery or construction of an isotropic negative μ material. Interest in Veselago's paper and LH materials begin to materialize when Professor Pendry at Imperial College demonstrated the first non-ferrite negative μ Metamaterial based on split ring resonators (SRRs) in 1998 Pendry's SRR was the cornerstone of the first bulk LH Metamaterial realization by a group at University of California, San Diego (UCSD) in 2000. So Metamaterial It"s an artificial and only material having simultaneously negative permittivity and permeability. Microstrip patch antennas are increasing in popularity for use in wireless applications due to their low-profile structure. Therefore they are extremely compatible for embedded antennas in handheld wireless devices such as cellular phones, pagers etc. The telemetry and communication antennas on missiles need to be thin and conformal and are often in the form of Microstrip patch antennas. Another area where they have been used successfully is in Satellite communication.

Due to having the negative refractive index it supports backward waves (antiparallel phase and group velocities) and does not obey some optical properties of nature. These special properties help Metamaterial to change the electric and magnetic property of electromagnetic waves passing through it and this helps in getting enhanced properties when applied to antenna design. Again as the structural average cell size of Metamaterial is less than one-fourth of the guided wavelength so it supports high degree of miniaturization. These Metamaterial antennas will be very suitable to use in WLAN (Both 2.4 and 5 GHz) because of its high performance and small size. Here metamaterial antenna using unit cell is proposed, designed and simulated using CST Microwave Studio software.

II. ANTENNA DESIGN

A. Unit Cell Design

Unit cells for designing RIS layer are S-shape structure. The S-RIS unit cell is shown in fig. 1. The unit cell is composed from top to bottom like as substrate followed by SRIS, substrate and ground respectively. The materials used in unit cell are substrate FR-4 with permittivity 4.3, tangent loss 0.0012, the ground and S-RIS is copper/perfect electric conductor. The dimensions of unit cell width and length are equal and denoted as 'Rw', the structure of S having dimensions denoted as 'S1', 'S2' and 'S3'. The boundary conditions are studied and shown in fig.1a. The top and bottom faces are assumed as PEC whereas left and right faces are assumed as PMC and the incident wave is passed over the unit cell with this assumption.

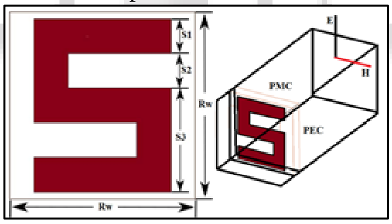

Fig. 1: Top view, of S-shape unit cell, a view of boundary conditions for EM analysis of S-RIS unit cell.

B. Proposed Rectangular patch antenna

The Rectangular Microstrip Patch Antenna is designed on FR-4 (Lossy) substrate. The parameter specifications of rectangular microstrip patch antenna are mentioned in table 1.

Specification	Dimensions	Unit
Dielectric Constant (εr)	4.3	
Loss Tangent (tan∂)	0.02	
Thickness (h)	1.6	mm
Operating Frequency	2.478 & 2.919	GHz
Length (L)	23.69	mm
Width (W)	30.71	mm
Cut Width	4.28	mm
Cut Depth	10	mm
Path Length	25.357	mm
Width of Feed	2.8	mm

Table 1: Rectangular Microstrip Patch Antenna Specifications

C. Design Specification

The Rectangular Microstrip Patch Antenna parameters are calculated from the formulas given below. Desired Parametric Analysis.

1) Calculation of Width (W)

$$W = \frac{1}{2f_r\sqrt{\mu_0\varepsilon_0}}\sqrt{\frac{2}{\varepsilon_r+1}} = \frac{c}{2f_r}\sqrt{\frac{2}{\varepsilon_r+1}} \quad (1)$$

Where

c = free space velocity of light

ε_r = Dielectric constant of substrate

2) The effective dielectric constant of the rectangular microstrip patch antenna

$$\varepsilon_{eff} = \frac{\varepsilon_r+1}{2} + \frac{\varepsilon_r-1}{2}\left(\frac{1}{\sqrt{1+\frac{12h}{w}}}\right) \quad (2)$$

3) The actual length of the Patch (L)

$$L = L_{eff} - 2L \quad (3)$$

Where

$$L_{eff} = \frac{c}{2f_r\sqrt{\varepsilon_{eff}}} \quad (4)$$

4) Calculation of Length Extension

$$\frac{\Delta L}{h} = 0.412\frac{(\varepsilon_{eff}+0.3)\left(\frac{W}{h}+0.264\right)}{(\varepsilon_{eff}-0.258)\left(\frac{W}{h}+0.8\right)} \quad (5)$$

Dimensional view of a rectangular microstrip patch antenna (RMPA), with a microstrip feed line is shown in Fig.2

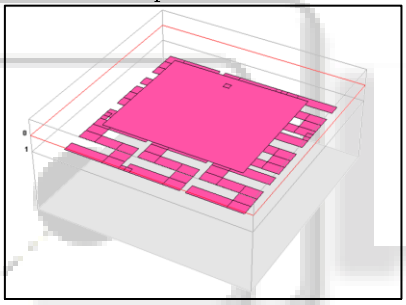

Fig. 2 Rectangular microstrip patch antenna with microstrip feed line

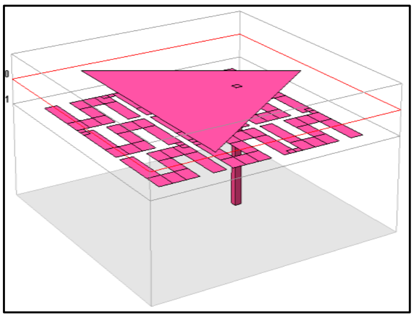

Fig. 3: Triangular microstrip patch antenna with microstrip feed line

The metallic patch essentially creates a resonant cavity, where the patch is the top of the cavity, the ground plane is the bottom of the cavity, and the edges of the patch form the sides of the cavity. The edges of the patch act approximately as an open-circuit boundary condition. Hence, the patch acts approximately as a cavity with perfect electric conductor on the top and bottom surfaces and a perfect “magnetic conductor” on the sides. This point of view is very useful in analyzing the patch antenna, as well as in understanding its behavior. Inside the patch cavity the electric field the electric field is essentially z directed and independent of the z coordinate. Hence, the patch cavity modes are described by a double index (m, n). For the (m, n) cavity mode of the rectangular patch the electric field has the form

$$E_z(x,y) = A_{mn}\cos\left(\frac{m\pi x}{L}\right)\cos\left(\frac{n\pi y}{W}\right) \quad (6)$$

III. Results and Discussions

A. Return loss

In the unloaded configuration good matching is obtained at 4.9GHz whereas poor matching is observed at the lower resonant frequencies. Thus, the antenna resonates at 4.9 GHz with the gain and bandwidth of 2.50 dBi and 9.18 % respectively. Hence, to obtain a good matching at lower frequencies, the square antenna is loaded with MSRR on the finite ground plane.

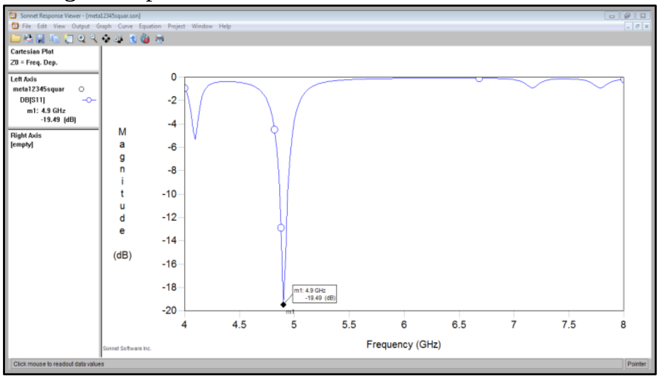

Fig. 4: depicts the return loss (S_{11}) characteristics of unloaded rectangular slotted microstrip patch

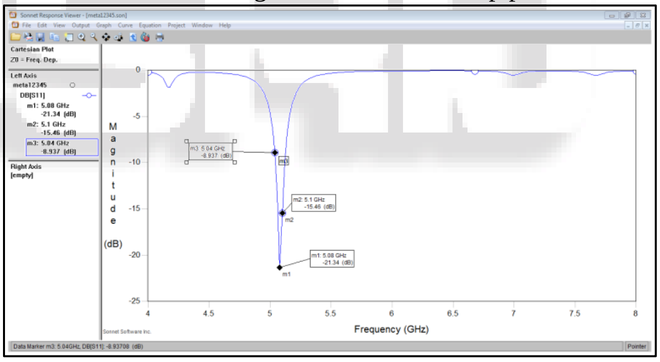

Fig. 5: depicts the return loss (S_{11}) characteristics of unloaded rectangular slotted microstrip patch

The return loss versus frequency plot for both S- RIS loaded square and triangle are shown in fig. 4 & 5. The square MSPA is found to be resonant at two frequencies 4.8 and 6.8GHz in C-band. In the case of S-RIS loaded triangle it is resonant with high bandwidth in the frequency range of 7-9.2GHz covering C-band and X-band frequencies respectively. This structure showed resonance at 7.6 GHz. The directive gain for S-RIS square MSPA is 5.9dBi at 4.8GHz whereas for S-RIS triangle MSPA the directive gain at 8.1GHz is 5.53dBi. It has been observed that both structures showed high gain at resonance frequencies. Square shape is resonant at two frequencies while triangular patch is resonant only one frequency with high bandwidth and gain. Both designs show miniaturization and high performance.

B. Smith Chart

The smith chart of the square metamaterial antenna has been shown in Figure 6 which depicts the impedance values (resistance as well as reactance) of the antenna at the marked frequency values. The almost real value of the impedance (with a very small reactance) at the resonance frequencies indicates the antenna requires lesser tuning to be done to match the antenna's impedance with the transmission line.

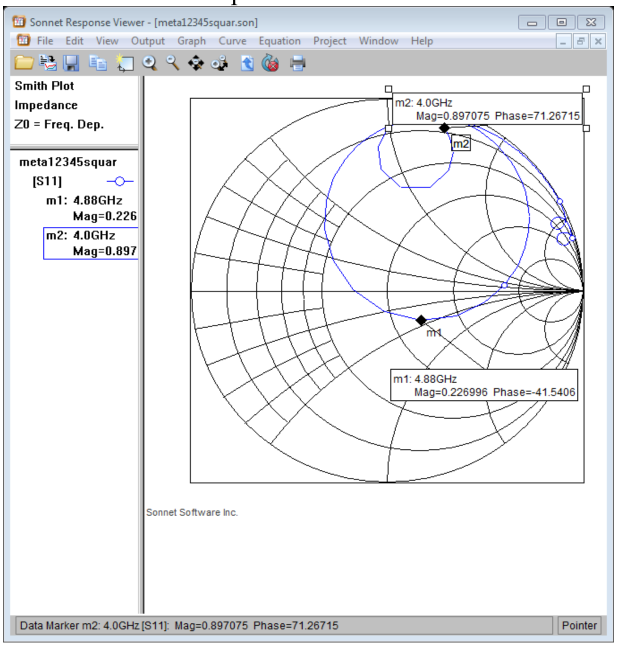

Fig. 6: Smith chart of the square metamaterial antenna

The smith chart of the triangular metamaterial antenna has been shown in Figure 7 which depicts the impedance values (resistance as well as reactance) of the antenna at the marked frequency values. The almost real value of the impedance (with a very small reactance) at the resonance frequencies indicates the antenna requires no more tuning to be done to match the antenna's impedance with the transmission line

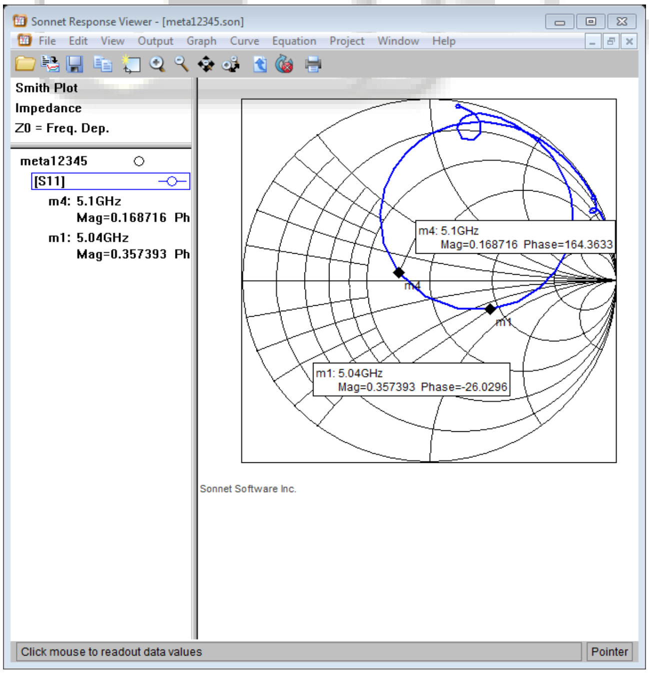

Fig. 7: Smith chart of the trianglular metamaterial antenna

C. *Surface Current Distribution*

Fig. 8 illustrates the simulated current distribution along the unloaded rectangular slotted microstrip patch antenna, in which the current flows at the perimeter whereas, there is almost no current flow path around the square.

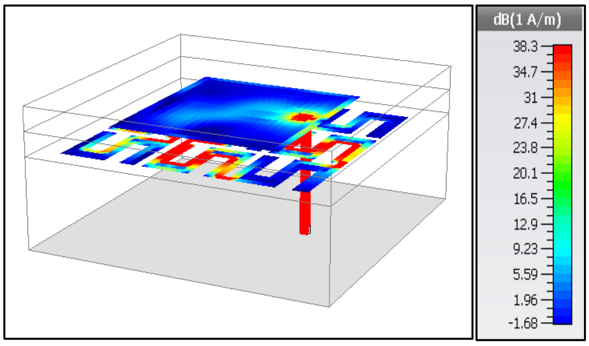

Fig. 8: Surface current distribution (A/m)

Fig. 9 depicts the simulated current distribution along the MSRR microstrip patch. At the lower resonant frequencies, the loading capacitor of MSRR reduces the mutual coupling and forces the current to flow around the perimeter of slot 1 in the circular manner. Thus, the uniform current distribution around the edges of both the slots increases the current path length on the patch. This reduces the resonant frequencies of the loaded antenna and contributes to the radiations.

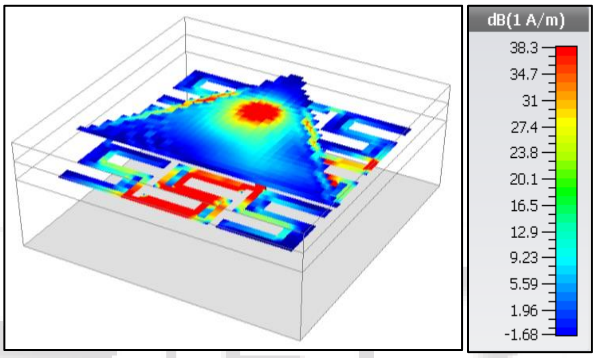

Fig. 9: Surface current distribution

IV. CONCLUSION

Electromagnetics of two patches of shapes square and triangle are analyzed with S-RIS using CST full wave simulation. The return loss versus frequency plot for both S-RIS loaded square and triangle are shown in fig. 2b. The square MSPA is found to be resonant at two frequencies 4.8 and 6.8GHz in C-band. In the case of S-RIS loaded triangle it is resonant with high bandwidth in the frequency range of 7-9.2GHz covering C-band and X-band frequencies respectively. This structure showed resonance at 7.6 GHz. The directive gain for S-RIS square MSPA is 5.9dBi at 4.8GHz whereas for S-RIS triangle MSPA the directive gain at 8.1GHz is 5.53dBi. It has been observed that both structures showed high gain at resonance frequencies. Square shape is resonant at two frequencies while triangular patch is resonant only one frequency with high bandwidth and gain. Both designs show miniaturization and high performance. Due to miniaturization and gain considerations proposed designs can be used to design and fabricate a phased array antenna for synthetic aperture radar (SAR) for dual band and high bandwidth applications. Miniaturization of array antenna leads to reduced weight of earth observation active payloads for airborne or space-borne platforms. It is further planned to use these structures for designing array antenna for UAV mounted SAR applications.

REFERENCES

[1] N. Herscovici, Z. Sipus and P. S. Kildal, "The Cylindrical Omnidirectional Patch Antenna," IEEE Trans. Antennas Propagat., vol. 49, no.12, pp.1746-1753, 2001.
[2] R. Porath, "Theory of miniaturized shorting-post microstrip antennas," IEEE Transactions on Antennas and Propagation, vol. 48, no. 1, January 2000, pp. 41-47.
[3] J. H. Lu and K. L. Wong, "Slot-loaded meandered rectangular microstrip antenna with compact dual frequency operation," Electronic Letters, vol. 34, May 1998, pp. 1048-1050.
[4] D. H. Schaubert, D. M. Pozar and A. Adrian, "Effect of microstrip antenna substrate thickness and permittivity," IEEE Transactions on Antennas and Propagation, vol. 37, no. 6, June 1989, pp. 677-682.
[5] D. Sievenpiper, L. Zhang, R. Broas, N.G. Alexopolous, and E. Yablonovitch, "High impedance electromagnetic surfaces with a forbidden frequency band," IEEE Transactions on Microwave Theory and Techniques, vol. 47, no. 11, Nov. 1999, pp. 2059–2074.